Journal of Experimental Nanoscience
Publication details, including instructions for authors and subscription information:
http://www.informaworld.com/smpp/title~content=t716100757

Multifunctional nanofibrous scaffold for tissue engineering

X. Yang[a]; K. R. Ogbolu[a]; H. Wang[a]
[a] Department of Chemical, Biomedical and Materials Engineering, Stevens Institute of Technology, Hoboken, NJ, USA

To cite this Article Yang, X. , Ogbolu, K. R. and Wang, H.(2008) 'Multifunctional nanofibrous scaffold for tissue engineering', Journal of Experimental Nanoscience, 3: 4, 329 — 345
To link to this Article: DOI: 10.1080/17458080701883707
URL: http://dx.doi.org/10.1080/17458080701883707

Journal of Experimental Nanoscience
Vol. 3, No. 4, December 2008, 329–345

Taylor & Francis
Taylor & Francis Group

Multifunctional nanofibrous scaffold for tissue engineering

X. Yang, K.R. Ogbolu and H. Wang*

Department of Chemical, Biomedical and Materials Engineering, Stevens Institute of Technology, Hoboken, NJ, USA

(*Received 20 October 2007; final version received 9 December 2007*)

In tissue engineering, scaffolds with multiscale functionality, especially with the ability to release locally multiple or specific bioactive molecules to targeted cell types, are highly desired in regulating appropriate cell phenotypes. In this study, poly (epsilon-caprolactone) (PCL) solutions (8% w/v) containing different amounts of bovine serum albumin (BSA) with or without collagen were electrospun into nanofibres. As verified by protein release assay and fluorescent labelling, BSA and collagen were successfully incorporated into electrospun nanofibres. The biological activity of functionalised fibres was proven in the cell culture experiments using human dermal fibroblasts. By controlling the sequential deposition and fibre alignment, 3D scaffolds with spatial distribution of collagen or BSA were assembled using fluorescently labelled nanofibres. Human dermal fibroblasts showed preferential adhesion to PCL nanofibres containing collagen than PCL alone. Taken together, multiscale scaffolds with diverse functionality and tunable distribution of biomolecules across the nanofibrous scaffold can be fabricated using electrospun nanofibres.

Keywords: nanofibres; multifunctional scaffold; electrospinning; tissue engineering; 3D microenvironment

1. Introduction

Tissue engineering has proven to be a promising alternative therapy in clinical practice [1] and can provide a well defined *in vitro* model for drug screening or tissue related studies [2]. In tissue engineering, a scaffold is normally used. Apart from its primary function as a temporary substrate for cells to attach and grow, more and more efforts in scaffold design are also made to provide the cells with instructive external cues to guide the tissue formation [3].

To maintain the appropriate phenotype of cells residing in the scaffold, it is desirable for the scaffold to recapitulate maximally the major features of native extracellular matrix (ECM) on a multiscale, from the composition, morphology, topography, to spatial organisation. Cells of *in vivo* tissues are either embedded in ECM fibres, or reside on the top of basement membrane consisting of tightly cross-linked ECM fibres with pores [4]. To this end, nanofibrous scaffold will be preferred

*Corresponding author. Email: hongjun.wang@stevens.edu

ISSN 1745–8080 print/ISSN 1745–8099 online

DOI: 10.1080/17458080701883707
http://www.informaworld.com

because of its similarity to ECM fibrils in both dimension and morphology. Indeed, the advantages of nanofibrous scaffold in promoting cell growth and maintaining proper phenotype have been demonstrated in a number of studies [5–8], which is a result of the synergistic effects of both nanotopography and chemical signalling [9, 10]. Several approaches are available to fabricate nanofibres including self assembly [11], phase separation [12, 5] and electrospinning [13–17].

Electrospinning, a high voltage driven spinning technique, receives particular attention due to its simplicity as well as the ability to produce nanofibres with similar dimensions as collagen fibrils in natural tissue matrix [17]. A variety of polymers such as PLGA, PLLA, PCL, PEOT-PBT, collagen, chitosan, or the composite materials [8, 15, 18–21] have been successfully electrospun into micro/nanosize fibres. Depending on the materials used and spinning conditions, fibrous meshes with microscale variation, for instance, in pore size and fibre diameter [22], can be produced. However, how to assemble nanofibres into a 3D scaffold with a maximum match to the native environment is still under investigation. In particular, many *in vivo* tissues and organs exhibit hierarchical layered structures with distinct ECM composition and arrangement in each layer. These anisotropic properties not only offer the cells distinct signalling information, but also provide the tissues with a unique mechanical performance to coordinate with the physiological requirement. For example, three distinctive layers (ventricularis, spongiosa, and fibrosa) are clearly recognised in the heart valve [23]. Densely packed collagen fibres are found in fibrosa layer to provide the predominant strength and stiffness, and prevent excessive stretching of valve. Spongiosa, composed of loosely arranged collagen and abundant hydrophilic glycosaminoglycans (GAG), lubricates the relative movement between ventricularis and fibrosa layers. Ventricularis is rich with elastin and shows radially aligned elastic fibres to enable the recoil and stretch of valve in response to the diastole and systole of heart. Thus, it is highly desirable to incorporate this hierarchical feature into multiscale design of elaborate scaffolds using electrospun nanofibres.

Synergistic regulation of cell behaviour by growth factors is critical for functional tissue formation [2, 24]. Supplement of soluble bioactive molecules in the culture medium can stimulate the cells; however, it is difficult to achieve a sustainable, separate and temporal stimulation to multiple cell types in the same culture. Inclusion of bioactive molecules directly into scaffolds is considered as a practical solution to the aforementioned matter [25]. Therefore, we hypothesise that specifically designed microenvironment can be formulated for different cells by combining the hierarchical spatial arrangement of nanofibres and incorporation of various bioactive molecules in the fibres.

Taken together, this study was aimed to demonstrate the feasibility of fabricating multifunctional nanofibrous scaffolds appropriate for engineering hierarchical tissue construct using electrospun nanofibres. Polycaprolactone (PCL), a biodegradable and biocompatible synthetic polymer [26, 27], was used as the base material to explore all the possibilities. Bioactive nanofibres containing either collagen type I, bovine serum albumin (BSA) or fibronectin (FN) were obtained by electrospinning the PCL mixture. Uniform distribution and bioactivity of these molecules in nanofibres were observed. The release of small molecules from nanofibres was controlled by the fibre diameter and initial loading amount. Nanofibre meshes with various topographical patterns caused correspondent cellular responses. Multilayered 3D scaffolds with

distinct distribution of bioactive molecules in between were successfully fabricated using PCL/Collagen and PCL/BSA nanofibres.

2. Materials and methods

2.1. *Materials*

Poly (epsilon-caprolactone) (PCL, Mw = 80,000), fluorescein isothiocyanate (FITC), TRITC conjugated phalloidin, and bovine serum albumin (BSA) were purchased from Sigma-Aldrich (St. Louis, MO). Collagen type I was purchased from Elastin Products Company (Owensville, MO). Fetal bovine serum (FBS) was purchased from American Type Culture Collection (ATCC, Manassas, VA). 1,1,1,3,3,3-hexafluoro-2-propanol (HFIP) was obtained from Oakwood products Inc (West Columbia, SC). All the other reagents and solutions were obtained from Invitrogen (Carlsbad, CA) except as indicated.

2.2. *Electrospinning and characterisation*

Collagen solution (8% w/v) and PCL solution (8% w/v) were prepared separately by dissolving collagen or PCL in HFIP. For collagen-PCL blended solution, 1 volume collagen and 1 volume PCL solutions were thoroughly mixed to obtain a homogeneous mixture. For PCL containing BSA or fibronectin (FN), a small amount of protein was added into the 8% PCL solution and mixed well. The solution was transferred to a 5 ml syringe attached with a tip-blunt capillary (inner diameter = 0.9 mm). A steady flow of the solution from the capillary spinneret was achieved using a syringe pump from KD Scientific (Holliston, MA), operating at a flow rate from 5 μL/min to 15 μL/min. A high voltage power supply from Gamma High Voltage Research (Ormond Beach, FL) was used to create electric field strength from 0.8 kV/cm to 2.0 kV/cm between the blunt tip capillary spinneret and a collection plate. The electrospinning distance between capillary spinneret to collection plate was between 7 cm and 10 cm. The typical electrospinning setup was shown in Figure 1. Electrospun fibres were collected on coverslips or aluminum foil for further use.

To characterise the electrospun nanofibre using a scanning electron microscope (SEM), fibres were collected on Si wafer and sputter-coated with gold. The coated fibres were examined with a LEO 982 FEG SEM. To determine the diameter of nanofibres, images of randomly selected five areas were captured and analysed by analysis software (NIS-elements BR 2.30 from Nikon).

2.3. *FITC-BSA conjugates and TRITC-BSA conjugates*

FITC or TRITC-BSA conjugates were prepared according to the instruction manual from the manufacturer. Briefly, 3.0 mg of FITC or TRITC was dissolved in 30 ml Hanks' Balanced Salt Solution (HBSS) to make 0.1 mg/ml solution. 0.8 g BSA was dissolved in 10 ml HBSS. The two solutions were mixed in the dark for 24 hrs at room temperature to form FITC-BSA or TRITC-BSA conjugates. After dialyzing to remove unreacted FITC or TRITC, the solution was lyophilised, and FITC or TRITC-conjugated BSA was obtained. It was then stored in the dark at 4°C for future use.

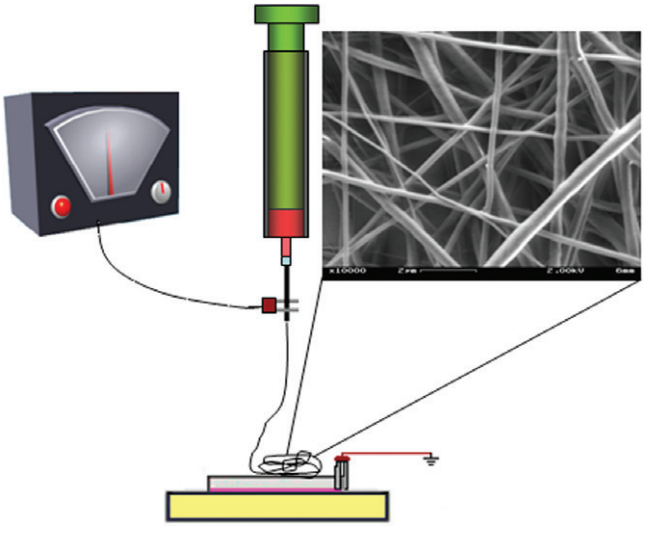

Figure 1. Illustration of the electrospinning setup. The inset is scanning electron microscopy (SEM) image of electrospun PCL nanofibres.

2.4. *Cell seeding and culture*

Human neonatal dermal fibroblasts (HDF, passage 1) were purchased from Cambrex Bio Science Walkersville, Inc. (Walkersville, MD). Cells were subcultured in FGM-2 medium (Cambrex) till passage 4–6 for use in the experiments. Cell splitting was performed when the monolayer cells reached 70–80% confluence.

To seed the cells onto electrospun fibres, cells were trypsinised, centrifuged and resuspended in Dulbecco's Modified Eagle Medium (DMEM) supplemented with 10% fetal bovine serum (FBS, ATCC, Manassas, VA) and 1% penicillin and streptomycin at a final concentration of 1×10^5 cells/mL. After seeding of HDF cells onto the electrospun fibres, cell-fibre constructs were cultivated in a humidified incubator at 37°C with 5% CO_2 for designated times.

2.5. *Cell morphology on electrospun fibres*

0.5 mL of HDF cell suspension (2×10^4 cells/mL) was seeded onto electrospun nanofibres collected on coverslips. After 24-hour culture at 37°C in a humidified atmosphere containing 5% CO_2, cells were washed with PBS and fixed in 3.7% formaldehyde in PBS for 5 minutes, then washed extensively in PBS. Cells were dehydrated with ethanol for 5 minutes, permeabilised with 0.1% Triton X-100 in PBS, and washed again in PBS. Cells were stained with a 50 μg/mL TRITC conjugated phalloidin (Sigma) solution in PBS for 40 minutes at room temperature, and then washed three times with PBS to remove unbound phalloidin conjugate. Then one drop of Vectashield mounting medium with DAPI was dispensed onto the coverslip. Cells were viewed at ex360 nm/em460 nm (DAPI) and ex540 nm/em570 nm (TRITC) using LCM 5 PASCAL with Axiovert 200 confocal microscope from Carl Zeiss.

For light microscopy observation, cell-cultured nanofibres were fixed in 1.5% glutaraldehyde-0.14 M cacodylate (pH = 7.4) and then stained with 0.1% methylene blue solution. Stained cells were observed either under a Nikon Stereomicroscope (SMZ1500) or with an inverted microscope (Trinoc Micromaster, Fisher Scientific Inc, Waltham, MA).

2.6. *BSA release from electrospun fibres*

For protein release studies, nanofibres were collected on aluminum foil. The collected nanofibre meshes were cut into discs (1.3 cm in diameter, $n = 3$) and placed in a 24-well plate with 1 ml phosphate buffer solution (PBS). The well plate was incubated at 37°C under gentle shaking (80 RPM). Samples (10 μL) were taken from the supernatant at 1 hour intervals for the first 24 hours and 24 hour intervals afterwards in the cumulative release. In continuous release experiments, supernatant was replaced with fresh PBS at each harvesting time point. The released BSA in harvested samples was measured with Lowry assay for those scaffolds with high BSA incorporation. For those scaffolds with low BSA incorporation, FITC-labelled BSA was used and the released BSA was detected by measuring the fluorescence intensity using a Synergy™ HT Multi-Detection Microplate Reader (BioTek Instruments Inc., Winooski, VT).

2.7. *Cell adhesion determined by MTS assay*

The cells attached on nanofibre meshes were monitored after overnight culture using the colorimetric MTS assay (CellTiter 96® Aqueous Assay, Sigma). The mechanism behind this assay is that metabolically active cells react with a tetrozolium salt in the MTS reagent to produce a soluble formazan dye that can be monitored at 490 nm. The cellular constructs were rinsed with PBS followed by incubation with 20% MTS reagent in serum free medium for 3 h. Thereafter, 100 L aliquots were pipetted into 96 well plates and the samples were read with a Synergy™ HT Multi-Detection Microplate Reader (BioTek Instruments Inc., Winooski, VT) at 490 nm. The tissue culture plastic (TCP) was used as internal control and pure PCL nanofibres were also included to compare the effect of ECM molecules on cell adhesion.

2.8. *Cryosectioning*

To visualise the spatial arrangement of different bioactive fibres or the distribution of cells in the fibres, samples were embedded in the sample freezing medium (Richard-Allan Scientific, Kalamazoo, MI) and plunge frozen at −50°C. The frozen samples were sectioned into thin slices (7–10 μm thick) at −25°C with a HM 550 cryostat from Richard Allen scientific. The slices were collected onto glass slides, air-dried at room temperature. For cell containing samples, the slides were stained with DAPI (Vector Laboratories Inc, Burlingame, CA). Then the slides were examined under the light microscope or Nikon Eclipse E1000 fluorescence microscope.

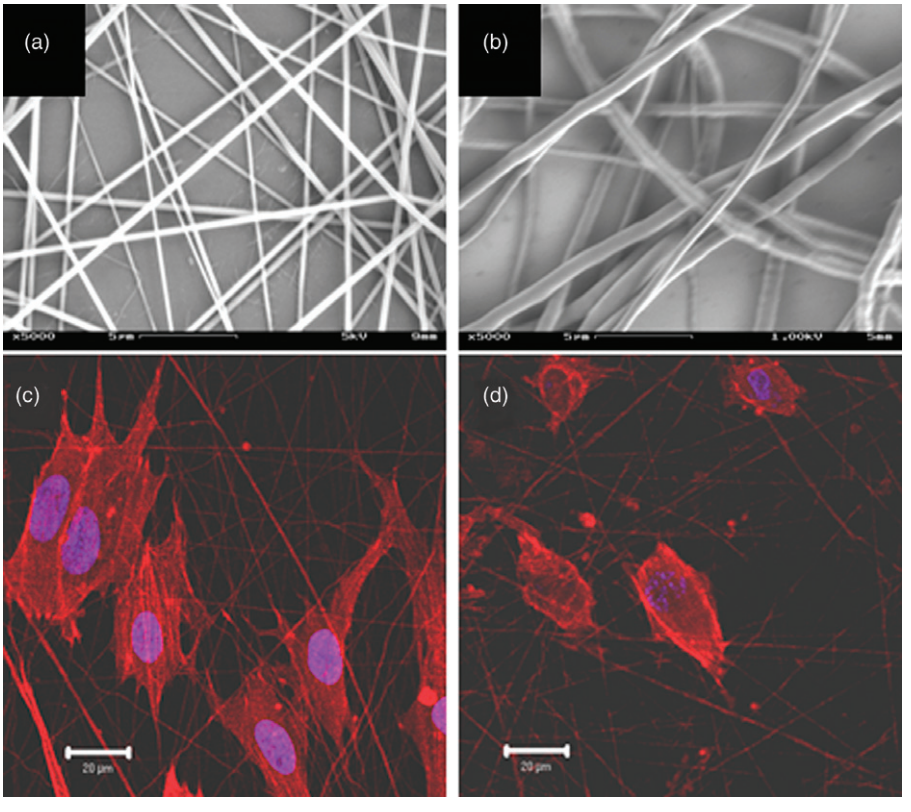

Figure 2. Growth of neonatal human dermal fibroblasts on electrospun nanofibres. SEM image of 1 : 1 (w/w) PCL/collagen fibres (a) and PCL fibres (b). Confocal microscopy images of cells cultured on PCL/collagen fibre meshes (c) and PCL meshes (d). Cells were stained with TRITC-phalloidin for F-Actin (red) and with DAPI for cell nuclei (blue). Scale bar: 20 μm.

2.9. *Statistical analysis*

Each experiment was repeated at least 3 times on different days and data were expressed as the mean ± SD. All the cytotoxicity and cell attachment measurements were collected in triplicate for each group. Unpaired student t-test was used to evaluate the significance between experimental groups. A value of $p < 0.05$ was considered to be statistically significant.

3. Results

3.1. *PCL-collagen nanofibres and cellular response*

To prepare collagen containing nanofibres, PCL solution (8% w/v) was mixed with different volumes of collagen solution (8% w/v) at a volume ratio of 1:1 and then electrospun into fibres using the experimental setup (voltage = 10 kV, collecting distance = 10 cm, and flow rate = 10 μl/min). The diameter of the obtained fibres ranged from 200 to 500 nm (Figure 2), which was smaller than that of pure PCL fibres (between 450 and 900 nm). The surfaces of both collagen/PCL and PCL nanofibres were smooth by

close examination using SEM (data not shown). To test if the inclusion of collagen into PCL nanofibres could facilitate cell attachment, human dermal fibroblasts were seeded onto nanofibrous meshes and cultured for 12 hours. Cell adhesion and spreading on these meshes were analysed by MTS assay and staining for F-actin. MTS results showed a significant increase (more than 30% increases) of the initial cell attachment onto PCL/collagen nanofibres compared to PCL alone. Staining for cytoskeleton protein, F-actin, showed that human dermal fibroblast spread nicely on the surface of PCL/collagen fibrous meshes with a spindle-like morphology (Figure 2(c)). In contrast, cells on PCL fibrous meshes retained limited spreading within the investigated time (Figure 2(d)), despite that prolonged culture could improve the cell stretch (data not shown).

3.2. *Inclusion of BSA in nanofibres and its release profile*

BSA, a model protein for growth factors, was successfully incorporated into the PCL nanofibres by electrospinning the PCL solution containing different amounts of BSA (BSA : PCL = 1 : 1, 1 : 60 to 1 : 600). Uniform distribution of BSA in the electrospun fibres was confirmed by using FITC-labelled BSA at a PCL/BSA ratio of 60 : 1 (Figure 3(a) inset). To determine the release of BSA from electrospun fibres, PCL/BSA nanofibrous meshes were incubated in PBS and the collected supernatant was analysed for the amount of BSA. A rapid release of BSA from PCL nanofibres was observed for those with 1 : 1 BSA/PCL ratio in the continuous release experiment. The majority of BSA (about 90%) was released within the first 3 hours in 1 : 1 BSA/PCL nanofibres, although the release of BSA was still detectable even after 24 hours (Figure 3(a)). In the cumulative release experiment, BSA release reached its plateau at about 8 hours and remained the same for rest of the experimental time (Figure 3(a)). The amount of BSA released into supernatant was proportional to the initial amount loaded into the PCL fibres (Figure 3(b)). When the BSA/PCL ratio decreased down to 1 : 60, the peak release started at approximately 24 hour in the continuous release experiment and lasted more than 6 days (Figure 3(b)). In addition, to correlate the BSA release profile with fibre diameter, 1 : 60 BSA/PCL nanofibres with two different average sizes (636.1 ± 211.8 nm and 322.6 ± 87.0 nm) were examined for BSA release. The results demonstrated that the thinner the fibres were, the earlier the peak release started in the continuous release experiments (Figure 3(c)). Two release phases were observed in BSA release from thick fibres: initial rapid release within 24 hours and a slow release afterwards. 24% of BSA was released from thick fibres within 24 hours in comparison to thin fibres (49%). By day 6, 85% of BSA was released from the thin fibre meshes in contrast to 62% from the thick ones. To release 85% of BSA from thick fibres, it took about 12 days in our experimental setup. The release amount per unit time decreased over the investigated time for both thin and thick fibres.

3.3. *Incorporation of fibronectin into nanofibres and its biological activity*

To investigate if the incorporated biomolecules into PCL fibres retain their biological activity, fibronectin (0.0125% w/w) was incorporated into the PCL fibres following a similar approach to BSA. Electrospun PCL nanofibres coated with 10 μg/mL fibronectin in PBS for 1 hour were used as positive controls and PCL nanofibres were used as negative controls. Fibroblasts were seeded and cultured on all three fibrous meshes for

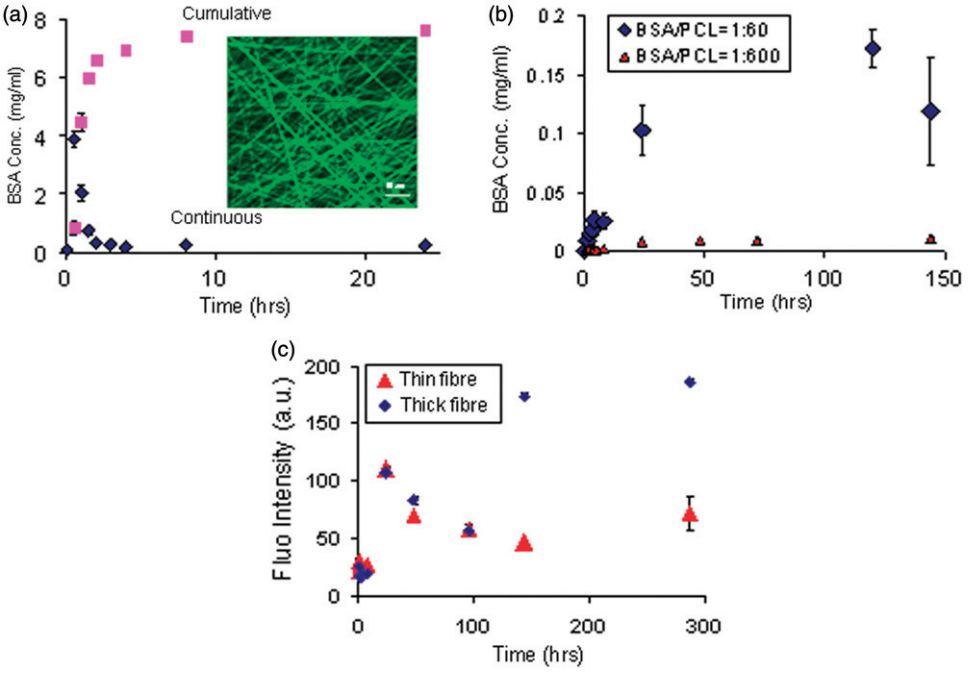

Figure 3. The release profile of bovine serum albumin (BSA) from electrospun PCL fibres. (a) BSA release from PCL/BSA (1 : 1, w/w) nanofibres into PBS, measured by Lowry assay. Inset, fluorescence image of the PCL/FITC-BSA. Scale bar: 10 μm. (b) BSA released into PBS from PCL nanofibres with 1 : 60 or 1 : 600 FITC-BSA/PCL ratios in the cumulative release experiments, determined by fluorescent intensity. (c) BSA released from nanofibres with different diameters in the continuous release experiments.

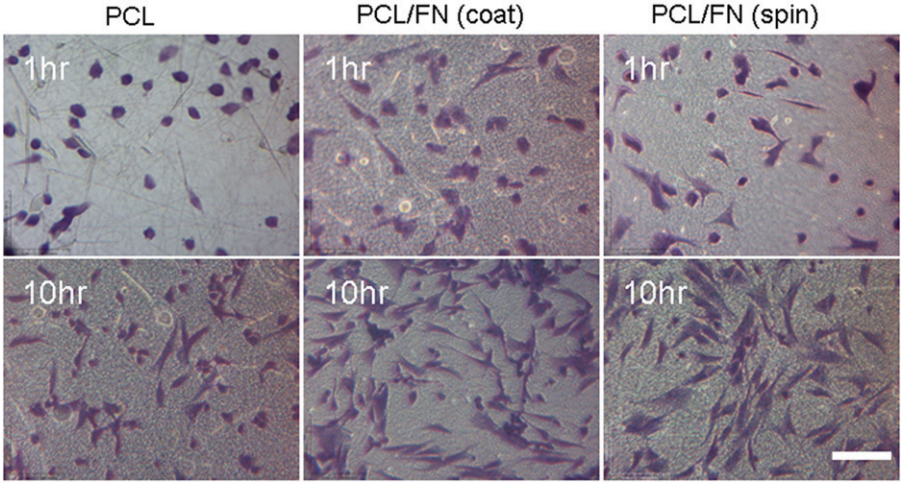

Figure 4. Cell morphology on different nanofibrous meshes at 1 and 10 hours after cell seeding. Cells were stained with methylene blue (blue). Scale bar: 100 μm.

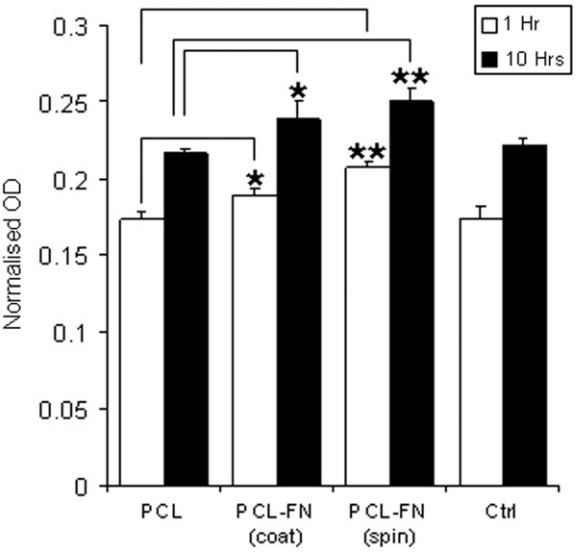

Figure 5. Cell adhesion to different nanofibre meshes, determined by MTS assay. Representative figure out of 3 separate experiments. $*P < 0.05$. $**$ $P < 0.001$. No significant difference was observed between PCL and TCP groups.

up to 10 hours. Methylene blue staining of the cell-fibre meshes illustrated differential cell response to the fibres (Figure 4). Compared to PCL only, both PCL/FN electrospun fibres PCL/FN coated fibres showed a rapid cell spreading from as early as 30 min up to 10 hours (Figure 4). On FN containing nanofibres, the majority of cells showed spindle-like morphology 10 hours after culture; in contrast, most cells still remained round shape or had minimal stretch on PCL only. Significant cell adhesion onto FN containing nanofibres was also observed early (as early as 1 hour after cell seeding) compared to PCL only or TCP, determined by MTS assay (Figure 5). With the culture extended to 10 hours, more cells attached to all the investigated surfaces, but still retained a similar adhesion trend. In addition, the PCL/FN electrospun fibres seemed more favorable to cell adhesion than PCL/FN coated fibres.

3.4. *Controllable spatial arrangement of nanofibres into various topographical patterns*

Alignment of ECM fibre is often observed in native tissue, leading to anisotropic mechanical performance. Figure 6 (top panel) shows the PCL/collagen/BSA-FITC nanofibres collected on glass coverslips with different electric field modification. Without modifying the electric field, PCL/collagen nanofibres randomly deposited on the collecting surface. By manipulating the intensity distribution of electric field on collecting surface, a gradient deposition of PCL/collagen nanofibres on the glass coverslip could be obtained. The alignment of PCL/collagen nanofibres was achieved by applying parallel grounded metal wires on the collecting surface described previously [28]. The aligned fibres were deposited across the wires, and by changing the angle of parallel wires the orientation of aligned fibres could be controlled. The cross-aligned fibres with

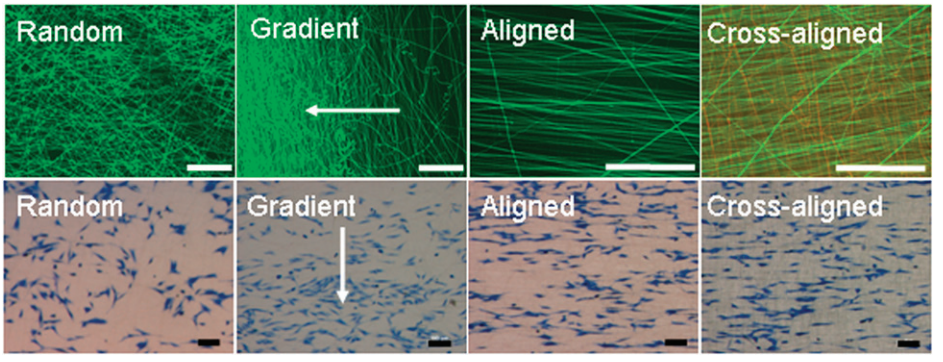

Figure 6. Cell growth on PCL/Collagen fibrous meshes with distinctive topographical patterns. Fluorescent images of nanofibres collected on glass coverslips (Top). Green fibres labelled with FITC-BSA and red fibres labelled with TRITC-BSA. Cells cultured overnight were stained with methylene blue (blue) (Bottom). Arrow indicates the gradient direction. Scale bar: 100 μm.

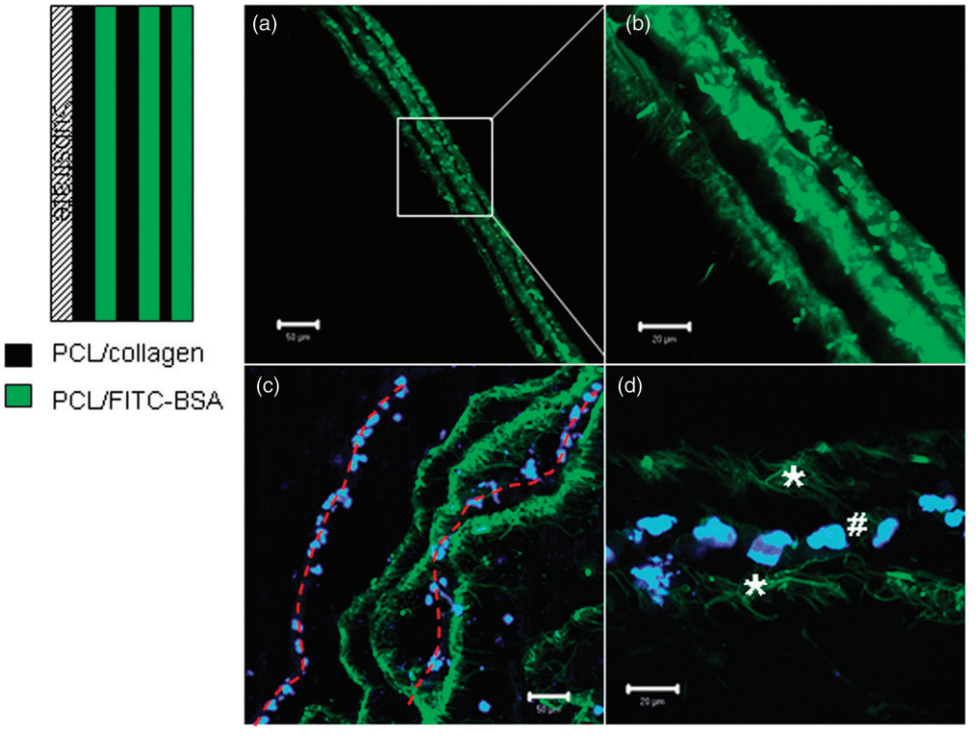

Figure 7. Fluorescence images of transverse sections of the nanofibrous structure. (a) and (b) Multifunctional scaffolds prepared by sequentially electrospinning of solutions as designated. (b) High magnification highlighting the clear layers. (c) Cell cultured in multifunctional scaffolds composed of PCL/collagen fibrous layer (outlined by red broken line) and PCL/BSA-FITC (green). High magnification (d) clearly showed cells attached onto PCL/collagen layers (#), but not onto PCL/BSA-FITC (*). Cell nuclei stained blue with DAPI. Scale bar: (a) and (c), 50 μm; (b) and (d), 20 μm.

two different compositions (PCL/Collagen/FITC-BSA, and PCL/Collagen/TRITC-BSA) were obtained by using parallel wires for the first TRITC fibres and then turning the wire pair 90° for the second FITC-fibre layer. Although the alignment was not perfect, cross alignment of two coloured fibres was clearly observed by overlaying the fluorescent images from green channel and red channel (Figure 6). So far, the controllable length scale for the fibre alignment is up to 2–3 cm, which can guide the distribution of cells and yield anisotropic mechanical properties. The fibroblasts, cultured on these nanofibre meshes overnight and stained with methylene blue, showed different distribution and spatial orientation in response to the various surface patterning (Figure 6, bottom panel). On aligned fibres cells also oriented along the nanofibre alignment direction. No obvious orientation was observed on the randomly collected fibres. Interestingly, a gradient cell distribution on the meshes was achieved when culturing cells on meshes with gradient nanofibre arrangement. Despite being only a few micrometers away, between the green and red-fluorescent layers, the cells cultured on the cross aligned bilayer nanofibres could only sense the nanofibre pattern directly contacted, but not that underneath.

3.5. *Anisotropic scaffolds with hierarchical structure*

To test the capability of manipulating sequential deposition of different layers of fibres into a spatially graded scaffold, a study was performed using PCL only and PCL/Collagen containing FITC-BSA. The sequence was shown in Figure 7 and sequentially deposited multiple layers were directly collected on aluminum foil (substrate). It was found that different nanofibre materials were comparably layered as designed sequence by examining the cross sections of collected scaffolds under a fluorescence microscope. By controlling the electrospinning time at a constant flow rate (10 μl/min), each layer could be altered with a designated thickness, from several micro meters to several tens of micro meters. A more confirmative result was obtained by using PCL nanofibres containing either TRITC-labelled BSA or FITC-labelled BSA for sequential deposition (Figure 8). Despite the fact that each layer was thinner on the circumferential edge of the multilayered scaffolds, the majority (5 cm in diameter in our experimental setup) remained uniform and kept the deposition sequence as designed.

The results also indicate that bioactive molecules can be incorporated into nanofibres and thereafter spatially arranged in a high order to form multifunctional scaffolds. In addition, it is intriguing to arrange cells with spatial distribution controlled by materials composition. Collagen containing nanofibres favored the attachment of fibroblasts; therefore we hypothesised that fibroblasts would primarily attach to PCL/collagen nanofibres instead of PCL nanofibres, and lead to the controllable spatial arrangement.

To test how the cell attachment to multifunctional scaffolds was affected by the presence of bioactive molecules, human dermal fibroblasts were seeded and cultured for 24 hours on scaffolds composed of collagen containing PCL fibres and PCL fibres. Examination of the cross-sections of cultured constructs showed that human dermal fibroblasts had a preferential attachment to collagen-containing nanofibres, as illustrated in Figure 7 (bottom). This preferential cell attachment is consistent with the observation that cells adhered and spread much faster on collagen-containing nanofibres. It is necessary to mention that layer separation, observed in Figure 5, is probably caused by

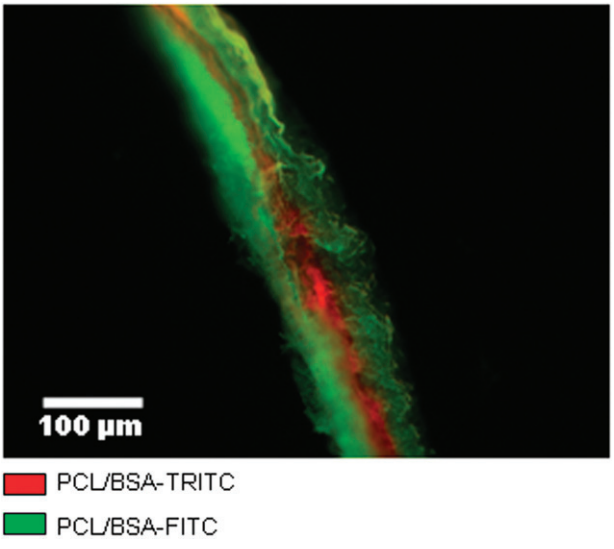

Figure 8. Fluorescence images of transverse sections of the three-layer nanofibrous scaffold. Red: PCL/BSA-TRITC. Green: PCL/BSA-FITC.

mechanical damage during sectioning; on the other hand, it indicates seeded cells did not adhere tightly onto PCL nanofibres to form an integral structure. With the extension of culture time up to 7 days, this separation was not seen any more as a result of newly synthesised ECM by cells (data not shown).

4. Discussion

The development of multifunctional scaffolds that can elicit the desirable biological responses such as adhesion, proliferation, differentiation, and especially phenotypic expression of residing cells is of particular interest in functional tissue engineering. The advantages of electrospun nanofibres in promoting cell adhesion and maintaining its phenotype as a result of its dimensional similarities to extracellular matrix (ECM) fibrils have been reported and explored as potential scaffolds for tissue engineering [8, 17]. This study demonstrated that bioactive nanofibres could be obtained by using electrospinning, and the anisotropic and hierarchical scaffolds with multifunctionality could be created by spatially arranging the bioactive nanofibres.

In this study, electrospun nanofibres of collagen blended PCL are considered superior to either pure PCL or collagen nanofibres by having both biological activity and mechanical stability. The biological superiority was demonstrated by its significantly improved fibroblast adhesion (more than 30% increase) and rapid spreading with spindle-like cell morphology (Figure 2). The selective attachment of dermal fibroblasts onto PCL/Collagen nanofibres instead of PCL nanofibres (Figure 7) further demonstrated the advantage of collagen as it can promote the cell-nanofibres interaction via cell

membrane integrin receptors such as $\alpha 2\beta 1$ [29–31]. Although pure collagen can be electrospun into nanofibres [30, 15] and proved favorable for cell attachment [32, 33], its rapid degradation leads to mechanical instability, and thus constrains its wide application as tissue engineering scaffolds [34]. The composite PCL/collagen nanofibres are considered to mimic the connective ECM better in both topology and composition with mechanical stability.

It has been shown that bioactive molecules can be incorporated into the nanofibres by mixing them into the polymer solution. More importantly, the bioactivity remains after processing as demonstrated in both collagen containing nanofibres and FN containing nanofibres (Figures 2, 4 and 5). Fibroblasts similarly adhered and spread on both PCL/FN electrospun nanofibres and the PCL nanofibres coated with FN. FN enhances fibroblast adhesion and spreading mainly through interaction with cell membrane integrins such as $\alpha 5\beta 1$ [35]. Although we did not stain for $\alpha 5\beta 1$, the comparable results between the two FN containing nanofibres suggest the bioactivity still remains intact after the electrospinning. This is very important evidence for further using electrospun fibres in creation of functional scaffolds. The retainment of biomolecule activity in electrospun fibres was also similarly reported in other studies [36, 37]. Thus, the inclusion of bioactive molecules in the nanofibres will allow us to better mimic the native ECM where numerous insoluble or soluble molecules anchor in the ECM fibres to mediate temporal cascades of cell function. Different from collagen, rapid release of BSA from the nanofibres would take place upon contact with medium. Several parameters have been found to influence the BSA release profile in this study. The BSA release from nanofibres greatly depends on the initial BSA amount loaded in nanofibres. At a high BSA density (1 : 1 BSA:PCL, w/w), the obtained burst release is consistent with a previous report [38], most likely as a result of concomitant release from both surface and inside of nanofibres. In contrast, at 1 : 60 BSA/PCL ratio, BSA release was significantly retarded (Figure 3). BSA rapidly released during the first a few hours probably comes from the surface of nanofibres, and that continuously released afterwards is from the inside of the nanofibres. The effect of fibre diameter on BSA release provided more evidence for this explanation, as more BSA released from thick fibres after the burst release (Figure 3(c)). The rapid initial release of BSA is probably due to BSA which is adsorbed or close to the surface of nanofibres and the large surface to volume ratio of the nanofibres. Upon contacting the release buffer, the superficial BSA rapidly dissolves into the release buffer accounting for the 'burst effect' [39, 40]. The slow release may be attributed to the diffusion of the BSA within the core of PCL nanofibres into the release buffer following the simple one dimensional diffusion model [41]. This diffusion is inversely proportional to the fibre diameter. The various BSA release profiles indicate that release of bioactive molecules can be tuned to achieve a programmable release by varying the initial drug loading, fibre diameter, spatial arrangement or fibre configuration.

Orientation of cells along the aligned fibres was observed in the culture of fibroblasts. Clearly, cell-nanofibre direct interaction is the determinant factor for controling cell orientation as only one direction was observed for the cells cultured on cross-aligned bilayer PCL/collagen fibres (Figure 6). This contact guidance inevitably includes the formation of focal adhesion composed of cytoskeletal proteins and integrin receptors [42],

and the involvement of integrin receptors can initiate the intracellular cascades to determine further cell function such as anchorage, traction for migration, differentiation, and possibly growth [35, 43, 44]. It has been reported that cell alignment could subsequently determine the orientation of newly deposited ECM [10, 45]. This implies that anisotropic new tissue formation can be controlled by an anisotropic scaffold originally designed. Our ongoing research will be devoted to investigating how nanofibres affect cell function and tissue formation. Although it was not investigated in this study, mechanical anisotropy of aligned fibres was previously reported in several studies [46–48]. A significant increase of aligned fibrous meshes in both Young's modulus (about 33 fold) and tensile modulus (about 5 fold) was measured compared to randomly collected meshes [46]. Ascribed to its anisotropic mechanical performance, biomechanical mimicking of soft tissue or musculoskeletal tissue using aligned fibres has shown promising results [46]. This free control of fibre alignment orientation can accommodate the requirements of native tissues with orientated ECM fibres changing from location to location.

Cells in native tissue not only experience the anisotropy from ECM fibre arrangement, but also respond to the varying chemistry from surrounding environment, which leads to the specific function and distinct property of individual tissue. The chemical stimulation can come from direct contact or from neighbors, and greatly depends on the spatial distribution. By changing the composition of nanofibres for electrospinning, multilayered scaffolds with specified chemistry and thickness for each layer were made as designed in this study (Figure 7). This demonstrates the potentials to use the layer-by-layer deposition approach towards creation of cell-specific 3D microenvironment by careful selection of nanofibre composition and incorporated bioactive molecules. This would be a useful tool to study cell–cell and cell–matrix interaction in a 3D environment similar to that *in vivo* but with more defined parameters. Interestingly, nanofibres containing bioactive component, for instance, collagen type I in this study, selectively promote cell attachment when competing with PCL nanofibres (Figure 7). This selectivity can be further enhanced by use of those molecules specifically interacting with special cell types [49, 50].

5. Conclusions

The present study has clearly demonstrated the feasibility of producing multiscale scaffolds with diverse functionality and tunable distribution of bioactive molecules across the scaffold using electrospun nanofibres. This multifunctional scaffold can offer the cells with specific and customised microenvironment depending on cell type. Ongoing studies focus on the incorporation of different growth factors into the scaffold and programmed release, and further investigate the effect on tissue formation.

Acknowledgements

The study was financially supported by the startup funds from Stevens. The authors would like to thank Dr. Arthur Ritter for his critical review and important discussion of this manuscript. Part of the results was presented in the NSTI Nanotech 2007 conference.

References

[1] R. Langer and J.P. Vacanti, *Tissue engineering*, Science 260 (1993), pp. 920–926.
[2] L.G. Griffith and M.A. Swartz, *Capturing complex 3d tissue physiology in vitro*, Nat. Rev. Mol. Cell. Biol. 7 (2006), pp. 211–224.
[3] M.P. Lutolf and J.A. Hubbell, *Synthetic biomaterials as instructive extracellular microenvironments for morphogenesis in tissue engineering*, Nat. Biotechnol. 23 (2005), pp. 47–55.
[4] G.A. Abrams, S.L. Goodman, P.F. Nealey, M. Franco, and C.J. Murphy, *Nanoscale topography of the basement membrane underlying the corneal epithelium of the rhesus macaque*, Cell Tissue Res. 299 (2000), pp. 39–46.
[5] K.M. Woo, J.H. Jun, V.J. Chen, J. Seo, J.H. Baek, H.M. Ryoo, G.S. Kim, M.J. Somerman, and P.X. Ma, *Nano-fibrous scaffolding promotes osteoblast differentiation and biomineralization*, Biomaterials 28 (2007), pp. 335–343.
[6] B.M. Min, G. Lee, S.H. Kim, Y.S. Nam, T.S. Lee, and W.H. Park, *Electrospinning of silk fibroin nanofibers and its effect on the adhesion and spreading of normal human keratinocytes and fibroblasts in vitro*, Biomaterials 25 (2004), pp. 1289–1297.
[7] Y. Ji, K. Ghosh, X.Z. Shu, B. Li, J.C. Sokolov, G.D. Prestwich, R.A. Clark, and M.H. Rafailovich, *Electrospun three-dimensional hyaluronic acid nanofibrous scaffolds*, Biomaterials 27 (2006), pp. 3782–3792.
[8] K.N. Chua, W.S. Lim, P. Zhang, H. Lu, J. Wen, S. Ramakrishna, K.W. Leong, and H.Q. Mao, *Stable immobilization of rat hepatocyte spheroids on galactosylated nanofiber scaffold*, Biomaterials 26 (2005), pp. 2537–2547.
[9] S. Patel, K. Kurpinski, R. Quigley, H. Gao, B.S. Hsiao, M.M. Poo, and S. Li, *Bioactive nanofibers: Synergistic effects of nanotopography and chemical signaling on cell guidance*, Nano. Lett. 7 (2007), pp. 2122–2128.
[10] J.H. Wang, F. Jia, T.W. Gilbert, and S.L. Woo, *Cell orientation determines the alignment of cell-produced collagenous matrix*, J. Biomech. 36 (2003), pp. 97–102.
[11] S. Zhang, *Fabrication of novel biomaterials through molecular self-assembly*, Nat. Biotechnol. 21 (2003), pp. 1171–1178.
[12] C.P. Barnes, S.A. Sell, E.D. Boland, D.G. Simpson, and G.L. Bowlin, *Nanofiber technology: Designing the next generation of tissue engineering scaffolds*, Adv. Drug Deliv. Rev. 59 (2007), pp. 1413–1433.
[13] A. Formhals, *Process and apparatus for preparing of artificial threads*, U.S.Pat. 1975504, 1934.
[14] T.A. Telemeco, C. Ayres, G.L. Bowlin, G.E. Wnek, E.D. Boland, N. Cohen, C.M. Baumgarten, J. Mathews, and D.G. Simpson, *Regulation of cellular infiltration into tissue engineering scaffolds composed of submicron diameter fibrils produced by electrospinning*, Acta Biomater. 1 (2005), pp. 377–385.
[15] J.A. Matthews, G.E. Wnek, D.G. Simpson, and G.L. Bowlin, *Electrospinning of collagen nanofibers*, Biomacromolecules 3 (2002), pp. 232–238.
[16] M. Michel, N. L'Heureux, R. Pouliot, W. Xu, F.A. Auger, and L. Germain, *Characterization of a new tissue-engineered human skin equivalent with hair*, In Vitro Cell Dev. Biol. Anim. 35 (1999), pp. 318–326.
[17] Q.P. Pham, U. Sharma, and A.G. Mikos, *Electrospinning of polymeric nanofibers for tissue engineering applications: A review*, Tissue Eng. 12 (2006), pp. 1197–1211.
[18] D. Li, G. Ouyang, J.T. McCann, and Y. Xia, *Collecting electrospun nanofibers with patterned electrodes*, Nano. Lett. 5 (2005), pp. 913–916.
[19] H. Yoshimoto, Y.M. Shin, H. Terai, and J.P. Vacanti, *A biodegradable nanofiber scaffold by electrospinning and its potential for bone tissue engineering*, Biomaterials 24 (2003), pp. 2077–2082.

[20] L. Moroni, R. Licht, J. de Boer, J.R. de Wijn, and C.A. van Blitterswijk, *Fiber diameter and texture of electrospun peot/pbt scaffolds influence human mesenchymal stem cell proliferation and morphology, and the release of incorporated compounds*, Biomaterials 27 (2006), pp. 4911–4922.
[21] X. Geng, O.H. Kwon, and J. Jang, *Electrospinning of chitosan dissolved in concentrated acetic acid solution*, Biomaterials 26 (2005), pp. 5427–5432.
[22] Q.P. Pham, U. Sharma, and A.G. Mikos, *Electrospun poly(epsilon-caprolactone) microfiber and multilayer nanofiber/microfiber scaffolds: characterization of scaffolds and measurement of cellular infiltration*, Biomacromolecules 7 (2006), pp. 2796–2805.
[23] F.J. Schoen and R.J. Levy, *Founder's award, 25th annual meeting of the society for biomaterials, perspectives. Providence, RI, April 28-May 2, 1999. Tissue heart valves: current challenges and future research perspectives*, J. Biomed. Mater. Res. 47 (1999), pp. 439–465.
[24] D.A. Frenz, W. Liu, J.D. Williams, V. Hatcher, V. Galinovic-Schwartz, K.C. Flanders, and T.R. Van de Water, *Induction of chondrogenesis: Requirement for synergistic interaction of basic fibroblast growth factor and transforming growth factor-beta*, Development 120 (1994), pp. 415–424.
[25] G. Wei, Q. Jin, W.V. Giannobile, and P.X. Ma, *The enhancement of osteogenesis by nano-fibrous scaffolds incorporating rhbmp-7 nanospheres*, Biomaterials 28 (2007), pp. 2087–2096.
[26] T.J. Corden, I.A. Jones, C.D. Rudd, P. Christian, S. Downes, and K.E. McDougall, *Physical and biocompatibility properties of poly-epsilon-caprolactone produced using* in situ *polymerisation: A novel manufacturing technique for long-fibre composite materials*, Biomaterials 21 (2000), pp. 713–724.
[27] H. Kweon, M.K. Yoo, I.K. Park, T.H. Kim, H.C. Lee, H.S. Lee, J.S. Oh, T. Akaike, and C.S. Cho, *A novel degradable polycaprolactone networks for tissue engineering*, Biomaterials 24 (2003), pp. 801–808.
[28] S.G. Ball, A.C. Shuttleworth, and C.M. Kielty, *Direct cell contact influences bone marrow mesenchymal stem cell fate*, Int. J. Biochem. Cell. Biol. 36 (2004), pp. 714–727.
[29] M. Tulla, O.T. Pentikainen, T. Viitasalo, J. Kapyla, U. Impola, P. Nykvist, L. Nissinen, M.S. Johnson, and J. Heino, *Selective binding of collagen subtypes by integrin alpha 1i, alpha 2i, and alpha 10i domains*, J. Biol. Chem. 276 (2001), pp. 48206–48212.
[30] P. Nykvist, H. Tu, J. Ivaska, J. Kapyla, T. Pihlajaniemi, and J. Heino, *Distinct recognition of collagen subtypes by alpha(1) beta(1) and alpha(2)beta(1) integrins. Alpha(1)beta(1) mediates cell adhesion to type xiii collagen*, J. Biol. Chem. 275 (2000), pp. 8255–8261.
[31] A.W. Orr, M.H. Ginsberg, S.J. Shattil, H. Deckmyn, and M.A. Schwartz, *Matrix-specific suppression of integrin activation in shear stress signaling*, Mol. Biol. Cell. 17 (2006), pp. 4686–4697.
[32] Y.R. Shih, C.N. Chen, S.W. Tsai, Y.J. Wang, and O.K. Lee, *Growth of mesenchymal stem cells on electrospun type i collagen nanofibers*, Stem Cells 24 (2006), pp. 2391–2397.
[33] K.S. Rho, L. Jeong, G. Lee, B.M. Seo, Y.J. Park, S.D. Hong, S. Roh, J.J. Cho, W.H. Park, and B.M. Min, *Electrospinning of collagen nanofibers: Effects on the behavior of normal human keratinocytes and early-stage wound healing*, Biomaterials 27 (2006), pp. 1452–1461.
[34] H. Wang, J. Pieper, F. Peters, C.A. van Blitterswijk, and E.N. Lamme, *Synthetic scaffold morphology controls human dermal connective tissue formation*, J. Biomed. Mater. Res. A. 74 (2005), pp. 523–532.
[35] S.K. Akiyama, *Integrins in cell adhesion and signaling*, Hum. Cell 9 (1996), pp. 181–186.
[36] E. Luong-Van, L. Grondahl, K.N. Chua, K.W. Leong, V. Nurcombe, and S.M. Cool, *Controlled release of heparin from poly(epsilon-caprolactone) electrospun fibers*, Biomaterials 27 (2006), pp. 2042–2050.
[37] S.Y. Chew, J. Wen, E.K. Yim, and K.W. Leong, *Sustained release of proteins from electrospun biodegradable fibers*, Biomacromolecules 6 (2005), pp. 2017–2024.

[38] J. Zeng, A. Aigner, F. Czubayko, T. Kissel, J.H. Wendorff, and A. Greiner, *Poly(vinyl alcohol) nanofibers by electrospinning as a protein delivery system and the retardation of enzyme release by additional polymer coatings*, Biomacromolecules 6 (2005), pp. 1484–1488.
[39] T. Govender, S. Stolnik, M.C. Garnett, L. Illum, and S.S. Davis, *Plga nanoparticles prepared by nanoprecipitation: Drug loading and release studies of a water soluble drug*, J. Control Release 57 (1999), pp. 171–185.
[40] R. Gref, Y. Minamitake, M.T. Peracchia, A. Domb, V. Trubetskoy, V. Torchilin, and R. Langer, *Poly(ethylene glycol)-coated nanospheres: Potential carriers for intravenous drug administration*, Pharm. Biotechnol. 10 (1997), pp. 167–198.
[41] B.D. Weinberg, R.B. Patel, A.A. Exner, G.M. Saidel, and J. Gao, *Modeling doxorubicin transport to improve intratumoral drug delivery to rf ablated tumors*, J. Control. Release 124 (2007), pp. 11–19.
[42] J. Meyle, H. Wolburg, and A.F. von Recum, *Surface micromorphology and cellular interactions*, J. Biomater. Appl. 7 (1993), pp. 362–374.
[43] S. Dedhar, E. Ruoslahti, and M.D. Pierschbacher, *A cell surface receptor complex for collagen type i recognizes the arg-gly-asp sequence*, J. Cell. Biol. 104 (1987), pp. 585–593.
[44] G. Zhao, O. Zinger, Z. Schwartz, M. Wieland, D. Landolt, and B.D. Boyan, *Osteoblast-like cells are sensitive to submicron-scale surface structure*, Clin. Oral Implants Res. 17 (2006), pp. 258–264.
[45] M.E. Manwaring, J.F. Walsh, and P.A. Tresco, *Contact guidance induced organization of extracellular matrix*, Biomaterials 25 (2004), pp. 3631–3638.
[46] W.J. Li, R.L. Mauck, J.A. Cooper, X. Yuan, and R.S. Tuan, *Engineering controllable anisotropy in electrospun biodegradable nanofibrous scaffolds for musculoskeletal tissue engineering*, J. Biomech. 40 (2006), pp. 1686–1693.
[47] T. Courtney, M.S. Sacks, J. Stankus, J. Guan, and W.R. Wagner, *Design and analysis of tissue engineering scaffolds that mimic soft tissue mechanical anisotropy*, Biomaterials 27 (2006), pp. 3631–3638.
[48] C. Ayres, G.L. Bowlin, S.C. Henderson, L. Taylor, J. Shultz, J. Alexander, T.A. Telemeco, and D.G. Simpson, *Modulation of anisotropy in electrospun tissue-engineering scaffolds: Analysis of fiber alignment by the fast fourier transform*, Biomaterials 27 (2006), pp. 5524–5534.
[49] L. Kam, W. Shain, J.N. Turner, and R. Bizios, *Selective adhesion of astrocytes to surfaces modified with immobilized peptides*, Biomaterials 23 (2002), pp. 511–515.
[50] S.E. Fischer, X. Liu, H.Q. Mao, and J.L. Harden, *Controlling cell adhesion to surfaces via associating bioactive triblock proteins*, Biomaterials 28 (2007), pp. 3325–3337.